



# CHORUS

This is the accepted manuscript made available via CHORUS. The article has been published as:

## Identification of Potential Photovoltaic Absorbers Based on First-Principles Spectroscopic Screening of Materials

Liping Yu and Alex Zunger

Phys. Rev. Lett. **108**, 068701 — Published 10 February 2012

DOI: [10.1103/PhysRevLett.108.068701](https://doi.org/10.1103/PhysRevLett.108.068701)

# Identification of potential photovoltaic absorbers based on first-principles spectroscopic screening of materials

Liping Yu\*

*National Renewable Energy Laboratory, Golden, Colorado 80401, USA*

Alex Zunger†

*University of Colorado, Boulder, Colorado 80309, USA*

There are numerous inorganic materials that may qualify as good photovoltaic (PV) absorbers, except that the currently available selection principle – focusing on materials with direct band gap of  $\sim 1.3$  eV made of earth abundant elements – does not provide compelling design principles even for the initial material screening. The conventional Shockley-Queisser efficiency criterion depends only on material’s band gap energy and ignores nonradiative recombination losses. Here we offer a calculable criterion of “spectroscopic limited maximum efficiency (SLME)” that can be used for initial screening based on intrinsic properties alone. It takes into account the band gap, the shape of absorption spectra and the material-dependent nonradiative recombination losses. High throughput first-principles quasiparticle calculations of SLME for  $\sim 260$  generalized  $I_pIII_qVI_r$  chalcopyrite materials identify over 20 high SLME materials, including the best known as well as previously unrecognized PV absorbers. It is found that some indirect gap materials may also be good for PV absorber. The strategy of combining advanced design principles with high-throughput first-principles evaluation of the spectroscopic input data could enable identification of hitherto overlooked, promising candidate materials in different optoelectronic technology areas.

PACS numbers: 81.05.Zx; 88.40.H-; 88.05.Bc; 78.20.-e; 78.20.Bh; 78.56.-a;

Most currently used solar-absorbing photovoltaic materials such as Si, GaAs, and  $CuInSe_2$  have been discovered accidentally, and were subsequently improved incrementally over tens of years, at significant R&D cost. Indeed, databases listing all previously made inorganic crystals contain a vast number of candidates (e.g.,  $\sim 135,500$  entries in Inorganic Crystal Structure Database (ICSD)[1]), yet almost none was ever systematically screened for potential PV significance. A contributing factor to this state of affairs is the absence of suitable “design principle” which can systematically drive materials screening. Heuristically established selection criteria of good absorbers have generally relied on favoring direct gap materials over indirect gap materials, a distinction based on the wave vector momentum of the initial and final states across the gap. This important distinction, motivated by the need to have strong absorption that enables the use of a small amount of material (i.e., thin films), is insufficient. Indeed, it fails to recognize the fact that some direct-gap materials might have a dipole-forbidden (DF) direct transition lower in energy than the dipole-allowed (DA) direct transition [2–5], so being direct does not guarantee good absorption. Likewise, indirect gap materials with properly positioned higher energy DA transitions might prove efficient. The classic and almost universally used predictor of PV cell efficiency due to Shockley and Queisser (SQ)[6] depends only on material’s band gap, offering but a very rough selection criterion for good PV materials – an optimal gap of  $\sim 1.3$  eV, no matter whether it is direct or indirect. This criterion alone has proven over the years to be

insufficient as numerous materials with this gap are poor PV absorbers.

PV device efficiency ( $\eta$ ) represents a complex convolution of thermodynamic, defect structure and optical characteristics, in addition to considerations such as fabrication, element abundance, toxicity and cost. Given the vast number ( $\sim 10^5$ ) of inorganic materials that may need to be eventually screened, we look for an initial filter based on the intrinsic spectroscopic and thermodynamic properties of the absorber, postponing scrutiny of imperfections (defects, fabrication-induced effects) and economic factors to after the initial field of candidates has been significantly narrowed down. We use the “spectroscopic limited maximum efficiency (SLME)” selection criterion, which accounts, within the thermodynamic “detailed balance” approach for (i) the existence of various energetic sequences of DA, DF and indirect band gaps (denoted by  $E_g^{da}$ ,  $E_g^{df}$  and  $E_g^i$  respectively), (ii) the specific shape of the absorption near the threshold, and (iii) the  $\Delta$ -dependent radiative recombination loss, where  $\Delta = E_g^{da} - E_g$ . The SLME captures the leading physics of absorption, emission and recombination characteristics, resolving a spread of different efficiencies for materials having the same gap. The spectroscopic quantities used in these three factors are obtained from first-principles quasiparticle calculations. It is illustrated here for  $\sim 260$  generalized  $I_pIII_qVI_r$  chalcopyrite materials in ICSD, revealing over 20 high SLME materials including the currently recognized best solar absorbers, yet adding a few previously unrecognized and potentially good PV absorbers.

We first classify materials into four “optical types”, based on the relative order of the direct-allowed, direct-forbidden, and indirect transitions, as illustrated schematically in Fig.1. “Optical type 1 (OT1)” is the case when the DA direct gap is the lowest energy transition and the next direct-but-forbidden transition is above it (i.e.,  $E_g^{da} \leq E_g^{df}$ ). “Optical type 2 (OT2)” is the case where the lowest transition is direct-but-forbidden, i.e., when  $E_g^{da} > E_g^{df}$ . Accordingly, “optical type 3 (OT3)” and “optical type 4 (OT4)” are two types of indirect gap materials, corresponding to cases with  $E_g^i < E_g^{da} \leq E_g^{df}$  and  $E_g^i < E_g^{df} < E_g^{da}$  respectively. Each of these four optical types has different characteristic absorption profile near threshold[7], depending on the order and energy separation between allowed and forbidden states. Subsequent, quantitative spectroscopic calculations (below) will demonstrate this classification on a class of materials.

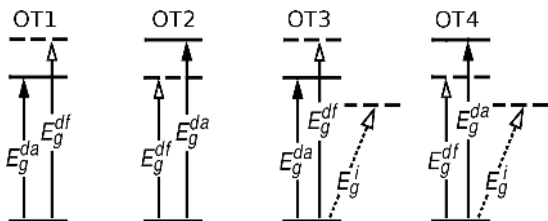


FIG. 1. Schematic diagrams of different optical types. Electric-dipole allowed (forbidden) direct optical transition is denoted by a line with an arrow pointing to solid (dashed) horizontal line. Indirect states are shown as laterally displaced dashed lines.

The SLME is generalized from the SQ limiting efficiency. The power conversion efficiency[8] of a thin film solar cell depends on the fraction of the radiative electron-hole recombination current ( $f_r$ ) and the photon absorptivity ( $a(E)$ )[9]. SLME improves upon the SQ efficiency formula in the description of both  $f_r$  and  $a(E)$ . SQ efficiency assumes  $f_r = 1$ , i.e., the radiative recombination is the only recombination process for all optical types of materials. This could be a good approximation for OT1 materials such as GaAs[10] where radiative recombination dominates. However for other types of materials where  $E_g^{da}$  is not the minimum band gap, the nonradiative recombinations (e.g., Auger recombination) is frequently much more significant[11, 12] (i.e.,  $f_r \ll 1$ ). Here in SLME, we approximate  $f_r = e^{-\Delta/kT}$ , where  $k$  is Boltzmann constant,  $T$  is the temperature and  $\Delta = E_g^{da} - E_g$ , near absorption threshold of a pure semiconductor [13]. This form we chose is inspired by the Boltzmann formula for the relative number densities of atoms in the different excited energy states in thermal equilibrium with a black-body radiation field. Clearly for OT1,  $\Delta = 0$  and  $f_c = 1$  as in SQ limit, while for other types of materials,  $\Delta > 0$  and  $f_c$  decreases exponentially as  $\Delta$ . It is expected that the radiative recombinations happen mainly across  $E_g^{da}$ . When  $E_g^{da}$  shifts up by  $\Delta$ ,

the radiative recombination rate is reduced by a factor of  $e^{-\Delta/kT}$ , but it still has to balance the incoming light in equilibrium. Therefore, a smaller  $f_r$  here actually is an indicator of higher nonradiative recombination loss and lower open circuit voltage. On the other hand, it also means that the more radiative recombination loss (larger  $f_r$ ) relative to nonradiative recombination loss, the better for PV absorber [14].

For photon absorptivity, SQ efficiency assumes a step-function absorptivity (i.e.,  $a(E) = 1$  for  $E \geq E_g$  and 0 for  $E < E_g$ ) for all materials. In SLME, we take  $a(E) = 1 - e^{-2\alpha(E)L}$ , where  $L$  is the thickness of the thin film with a zero-reflectivity front surface and unity-reflectivity back surface[15]. The  $\alpha(E)$  is the calculated absorption coefficient from first principles. Thus, different optical types also manifest different  $a(E)$  through their absorption coefficient  $\alpha(E)$ . In addition, SLME also uses the standard AM1.5G flat-plate solar spectrum at 25°C[16].

The required inputs for SLME calculations are the band gaps and absorption spectrum. These quantities are calculated (see details in [17]) based on GW approximation[18] for electron’s self-energy. The method has been widely and successfully applied in first-principles quasiparticle electronic-structure calculations for many materials[19–21]. It enables direct comparison with experimental photoemission or inverse-photoemission measurements. Out of many GW schemes, we choose to apply GW approximation perturbatively on the top of the wavefunctions and energy eigenvalues calculated from a generalized Kohn-Sham scheme with the hybrid exchange-correlation functional HSE0[22], i.e.,  $G_0W_0$ +HSE06 [23]. Within this scheme, it has been shown that for a variety of materials (even those with shallow  $d$  states), the calculated excited-state properties such as band gaps agree well with experiment[23, 24]. Our  $G_0W_0$ +HSE06 predicted minimum band gaps for some I-III-VI (I=Cu,Ag) compounds have an average error of less than 12% with respect to experiments (see Figure S1a[17]).

We illustrate our foregoing ideas by considering generalized I-III-VI chalcopyrite group materials, i.e.,  $I_p\text{III}_q\text{VI}_r$ , where we use I = Li, Na, K, Rb, Cs, Cu, Ag; III = B, Al, Ga, In, Tl, Sc, Y; VI = O, S, Se, Te; and any stoichiometric ratios ( $p:q:r$ ) reported in ICSD. This group includes the well-known PV absorbers such as  $\text{CuInSe}_2$ ,  $\text{CuGaSe}_2$  and their solid solution  $\text{Cu(In,Ga)Se}_2$ . We consider here 256 reported compounds of this group [17], covering most of stoichiometries and structure types that have been documented in ICSD. So far, most studies of ordinary chalcopyrites have focused on compounds with (1:1:2) stoichiometry[25]. Fig.S2[17] shows the distribution of all integer stoichiometries reported in ICSD for this group, indicating that in addition to the most popular (1:1:2), some other stoichiometries, like (3:1:3), (1:3:5) etc, are also rather common but their physical material

properties are mostly unknown [26]. As will be seen below, some compounds with non-(1:1:2)-stoichiometry could be also good for PV absorber.

The calculated GW band gaps of considered 256 compounds are given in the supplementary Table S1[17]. Fig.2 shows the GW gaps of 215 compounds[27] classified into four optical types. Some clear trends emerge here: (i) Within the same structure type, the band gap of materials decreases with increasing atomic number of one atom when the other two atoms are held fixed. For instance, for OT1 materials,  $E_g^{da}(\text{LiAlSe}_2) > E_g^{da}(\text{LiGaSe}_2) > E_g^{da}(\text{LiInSe}_2)$ . (ii) The optical types can change if the stoichiometry changes within the same element set. For example,  $\text{Cu}_3\text{TlSe}_2$  (OT3)  $\rightarrow$   $\text{Cu}_5\text{TlSe}_3$  (OT4)  $\rightarrow$   $\text{Cu}_7\text{TlSe}_4$  (OT1)  $\rightarrow$   $\text{CuTlSe}_2$  (OT2). (iii) For the same compound, the minimum band gap ( $E_g$ ) may vary by more than 2 eV in different crystal structures, whether or not the optical type changes. For example, for  $\text{NaTlO}_2$ ,  $E_g = 0.07\text{eV}$  in the space group of #225 (OT4) and  $2.27\text{eV}$  in #166 (OT2). For  $\text{LiInO}_2$  (OT3),  $E_g = 0.19\text{ eV}$  and  $4.05\text{ eV}$  respectively in two structures of same space group (#141). (iv) All reported  $\text{I}_3\text{III}_1\text{VI}_3$  materials have small differences (less than 0.2 eV) between  $E_g^{df}$ ,  $E_g^{da}$  and  $E_g^i$ , except  $\text{Li}_3\text{BO}_3$  which has 0.43 eV difference between  $E_g^{da}$  and  $E_g^{df}$ .

Different optoelectronic applications may require different optical types. For examples, transparent conductors benefit from a large transparency band gap ( $E_g^{da}$ ), while the gap that decides dopability (the minimum gap  $E_g$ , whether allowed or not) can be much lower[28, 29]. Thus, OT2 with small  $E_g^{df}$  and large  $E_g^{da}$ , and indirect gap materials (OT3 or OT4) with a small  $E_g^i$  and large enough  $E_g^{da}$  are preferred. Table S2[17] lists 26 such potential TCO materials with  $3\text{ eV} < E_g^{da} < 5\text{ eV}$  and  $E_g^{da} - E_g > 0.5\text{ eV}$  found in Fig.2, including well-known TCs such as  $\text{Cu}_1\text{III}_1\text{O}_2$  (III= Al, Ga, In)[30, 31]. For light emitter and scintillator, OT1 with large dipole matrix element across  $E_g^{da}$  is preferred.

The SLME definition shows that it depends also on thin film thickness ( $L$ ). Fig.3 illustrates that SLME increases as  $L$  increases. At very small  $L$ , due to weak absorptivity, the SLME of  $\text{AgInTe}_2$  and  $\text{Cu}_7\text{TlS}_4$  and their SLME difference are also small. At very large  $L$ , the SLME of these two OT1 materials approach the same SQ efficiency limit since they have the same  $E_g$ , and hence the SLME difference due to different characteristic absorption spectra also disappears. Therefore, to include the effect of the material-dependent spectroscopic properties in SLME, a reasonable size of  $L$  should be used and we choose here  $L = 0.5\mu\text{m}$ .

Fig.4 shows calculated SLME for generalized I-III-VI thin film materials with thickness  $L = 0.5\mu\text{m}$  resolved into ‘‘optical Types’’. The SQ efficiency limit under AM1.5G solar spectrum is shown as the solid line and depends universally only on  $E_g$  for all optical types, pre-

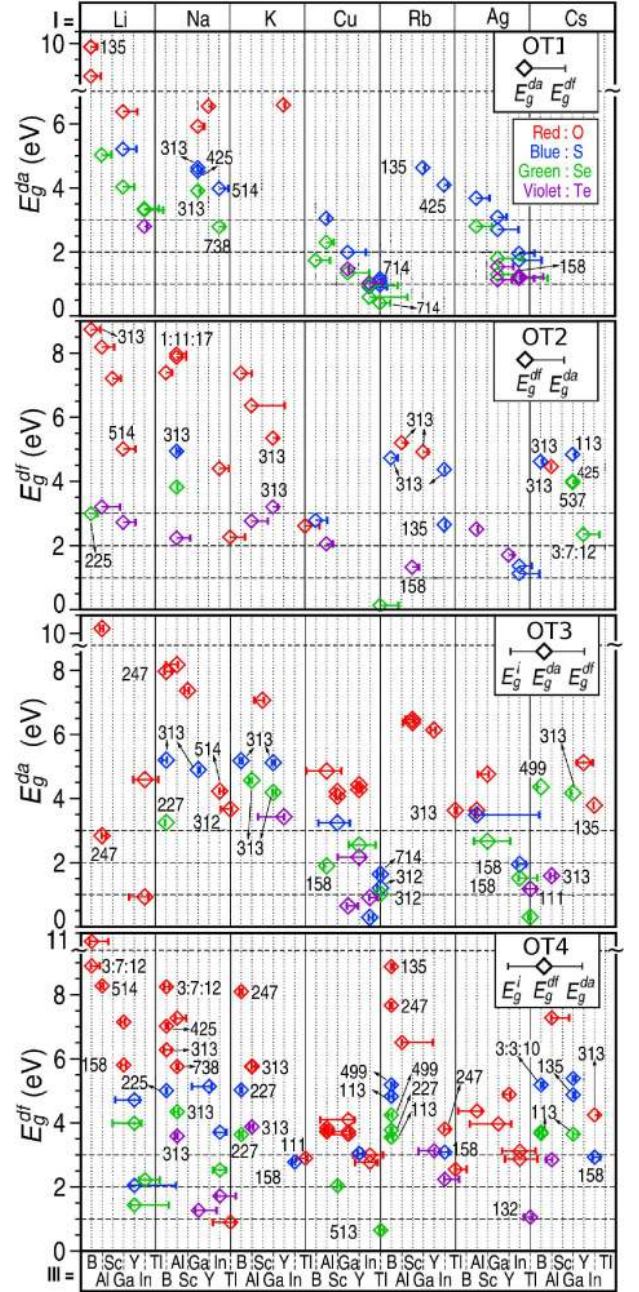


FIG. 2. (Color online) GW band gaps of generalized I-III-VI chalcopyrite materials. At each point, the right horizontal bar represents  $|E_g^{da} - E_g^{df}|$ , and the left horizontal bar corresponds to  $E_g^{da} - E_g^i$  (OT3) or  $E_g^{df} - E_g^i$  (OT4). Each block separated by vertical dotted lines has a width of 0.5 eV. All stoichiometric ratios other than (1:1:2) are marked. Different materials with same chemical formula are not distinguished.

dicting that the best gap for a PV absorber is 1.34 eV, at which  $\eta_{SQ} = 33.7\%$ . Our approach reveals instead a broad distribution of  $\eta$  values even around the same  $E_g$ , depending on the ‘‘optical types’’ and absorption spectra. For instance,  $\text{AgInTe}_2$ ,  $\text{Cu}_7\text{TlS}_4$  and  $\text{CuYTe}_2$  have almost same minimum gap(1.17eV), but their SLMEs vary



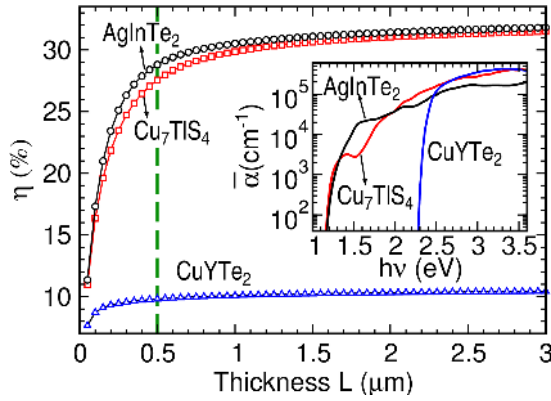


FIG. 3. (Color online) The SLME as a function of thin film thickness for  $\text{AgInTe}_2$ ,  $\text{Cu}_7\text{TlS}_4$  and  $\text{CuYTe}_2$ . The vertical dash line indicates the thickness adopted in Fig.4. The inset shows their absorption spectra.

significantly, being 27.6%, 22.6% and 7.5% respectively. From the inset of Fig.3, it can be seen that the SLME difference between  $\text{AgInTe}_2$  and  $\text{Cu}_7\text{TlS}_4$  originates from different onset absorption spectra. For  $\text{CuYTe}_2$ , the  $E_g^{da}$  is about 1 eV larger than  $E_g$ , i.e.,  $\Delta = 1\text{eV}$ , and hence the nonradiative recombination loss dominates. This large  $\Delta$  leads to a much smaller overlap between absorption spectrum and solar spectrum. Hence, although the absorption near  $E_g^{da}$  (2.2 eV) is very strong in  $\text{CuYTe}_2$ , the SLME is still rather small. Therefore, a material with the minimum gap being around 1.0-1.5 eV does not necessarily mean it is a good PV absorber.

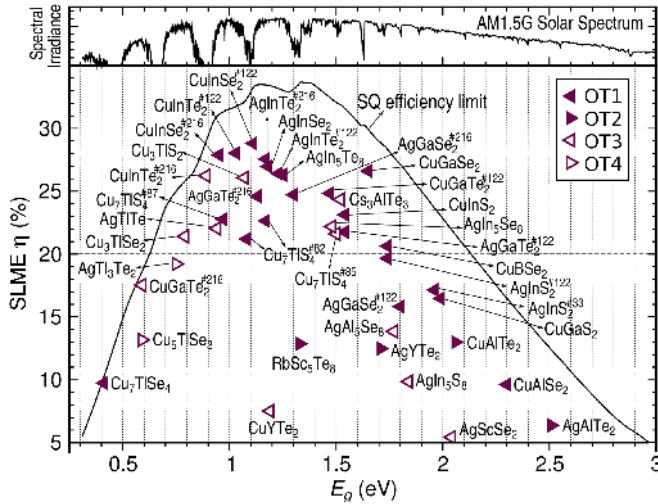


FIG. 4. (Color online) SLME ( $\eta$ ) for generalized I-III-VI chalcopyrite materials at  $L = 0.5\mu\text{m}$ . The compounds with SLME  $< 5\%$  are not shown. The shown space group number (superscript) is used to distinguish different materials with same chemical formula.

From Fig.4, we can find that there are about 25 materials with SLME higher than 20% (see Table S3[17] for

detail). These high SLME materials have the band gaps ranging from 0.8 eV to 1.75 eV. Most of them – 18 out of 25 – are OT1. Seven of them are OT3. None of them has been found to be OT2 or OT4. The common character among these OT3 materials is that  $E_g^i$  is only slightly smaller than  $E_g^{da}$ , i.e., small  $\Delta$ . For example,  $\Delta = 0.07\text{eV}$  for  $\text{Cs}_3\text{AlTe}_3$ , and  $0.14\text{eV}$  for  $\text{Cu}_3\text{TlS}_2$ . Relative to OT1, this small  $\Delta$  may cause higher joint density of states (DOS) at energies near  $E_g^{da}$  and good dispersive bands around the gap edges, and hence could lead to stronger onset optical absorption. OT2 and OT4 materials, both with  $E_g^{df} < E_g^{da}$ , are least favorable for PV absorbers.

Our predicted high SLME materials in Fig.4 include current best thin film solar absorber materials used in industry such as  $\text{CuInSe}_2$ ,  $\text{CuGaSe}_2$  and  $\text{CuInS}_2$ . The top candidate is  $\text{CuInSe}_2$ [32]. Its SLME is 28.8% at  $L = 0.5\mu\text{m}$ , which exceeds the highest efficiency (20%) currently reported in experiments[33–35]. It is gratifying that the SLME criterion flashes out in addition to  $\text{CuInSe}_2$ ,  $\text{CuGaSe}_2$  and  $\text{CuInS}_2$ , also seven other high SLME materials, namely,  $\text{CuInTe}_2$ [36],  $\text{CuGaTe}_2$ [37],  $\text{AgInS}_2$ [38],  $\text{AgInSe}_2$ [39],  $\text{AgInTe}_2$ [40],  $\text{AgGaSe}_2$ [41], and  $\text{AgGaTe}_2$ [42], that have been found experimentally to be reasonable solar absorbers but are much less studied. Most of these previously recognized absorber materials within this group have (1:1:2) stoichiometry. Here we find that materials with other stoichiometries (e.g.,  $\text{AgIn}_5\text{Se}_8$ ,  $\text{Cs}_3\text{AlTe}_3$ ) can also have high SLME.

Interestingly, it is found that all six high-SLME Cu-Tl-VI materials (i.e., four  $\text{Cu}_7\text{TlS}_4$ , one  $\text{Cu}_3\text{TlS}_2$  and one  $\text{Cu}_3\text{TlSe}_2$ ) are in non-(1:1:2)-stoichiometry and contain only Tl of +1 oxidation state [43]. Since Tl is highly toxic, these Tl-containing materials might be specifically disfavored in practical application. However, it indeed suggests that other similar high-SLME materials may be derived by replacing  $\text{Tl}^{1+}$  with other nontoxic element in 1+ oxidation state. Table S4 [17] summarized our identified  $\text{Cu}_p(\text{I,II})_q\text{VI}_r$  materials that have SLME more than 20%, not involving Tl.

In summary, the strategy adopted in this work involved: (i) recognizing a broad partitioning of materials into different “optical types”; (ii) developing generalized “design principle” constituting a new efficiency metric SLME that considers different optical types and material-dependent nonradiative recombination loss; and (iii) testing the idea on a couple of hundred generalized I-III-VI chalcopyrites using high-throughput first-principles spectroscopy calculations and identifying potential PV absorber materials that from the point view of absorption are comparable to  $\text{CuInSe}_2$  in the same group. Our identified high SLME materials within this group include almost all currently using PV absorber materials as well as those that have been testified to be promising in experiment. It suggests that as an initial filter, our proposed SLME is indeed very effective for selecting good potential PV absorber materials [44].

## ACKNOWLEDGMENTS

We thank Dr. Julien Vidal and Dr. Stephan Lany from NREL for illuminating discussions. We also acknowledge Professor Alex Freundlich from University of Houston for comments on the Shockley-Queisser methodology, Professor Douglas A. Keszler and Dr. Robert Kykyneshi from Oregon State university for the valuable discussion on the choice of thin film thickness for SLME. LY also thanks Dr. Vladan Stevanovic from NREL for providing the draft python script for generating VASP POSCAR from CIF file. This work was supported by U.S. DOE, Office of Science, Energy Frontier Research Centers, and used capabilities of the NREL Computational Sciences Center supported by U.S. DOE EERE, under grant No. DE-AC36-08GO28308 to NREL.

\* yuliping@gmail.com

† alex.zunger@gmail.com

- [1] F. Karlsruhe, “Inorganic crystal structure database,” <http://www.fiz-karlsruhe.de/icsd.html>.
- [2] J. Dahl and A. Switendick, *J. Phys. Chem. Solids* **27**, 931 (1966).
- [3] D. Fröhlich, R. Kenkies, and R. Helbig, *Phys. Rev. Lett.* **41**, 1750 (1978).
- [4] M. Stapelbroek and B. Evans, *Solid State Commun.* **25**, 959 (1978).
- [5] A. Walsh, J. L. F. Da Silva, S.-H. Wei, C. Korber, A. Klein, L. F. J. Piper, A. DeMasi, K. E. Smith, G. Panaccione, P. Torelli, D. J. Payne, A. Bourlange, and R. G. Egdell, *Phys. Rev. Lett.* **100**, 167402 (2008).
- [6] W. Shockley and H. J. Queisser, *J. of Appl. Phys.* **32**, 510 (1961).
- [7] In OT1, the absorption takes off rapidly with increasing photon-energy above the threshold, whereas in other three types there is an incubation energy range before the absorption takes off.
- [8] M. A. Green, *Third Generation Photovoltaics: Advanced solar energy conversion* (Springer, 2003).
- [9] The power conversion efficiency  $\eta$  of a solar cell is defined as  $\eta = P_m/P_{in}$ , where  $P_{in}$  is the total incident solar energy density, and  $P_m$  is the maximum output power density which can be obtained by numerically maximizing the product of current density  $J$  and voltage  $V$ . For a solar cell illuminated under the photon flux  $I_{sun}$  at temperature  $T$  that behaves as the ideal diode,  $J$  and  $V$  follow  $J = J_{sc} - J_0(1 - e^{eV/kT})$  [8]. The first term is the short-circuit current density  $J_{sc}$  given by  $J_{sc} = e \int_0^\infty a(E)I_{sun}(E)dE$ , where  $e$  is the elementary charge and  $a(E)$  is the photon absorptivity. The second term is the reverse saturation current  $J_0 = J_0^{nr} + J_0^r = J_0^r/f_r$ , corresponding to the total (non-radiative  $J_0^{nr}$  plus radiative  $J_0^r$ ) e-h recombination current at equilibrium in the dark, where  $f_r$  is the fraction of the radiative recombination current. As required by the principle of detailed balance, the rates of emission and absorption through cell surfaces must equal in equilibrium in the dark. Thus,  $J_0^r$  is easily calculated from the rate at which black-body photons from the surrounding thermal bath are absorbed through the front surface [15], i.e.,  $J_0^r = e\pi \int_0^\infty a(E)I_{bb}(E,T)dE$ , where  $I_{bb}$  is the black-body spectrum at  $T$ . Therefore, the maximum  $\eta$  of a material can be evaluated once we know how to calculate/model its  $a(E)$  and  $f_r$ .
- [10] I. Schnitzer, E. Yablonovitch, C. Caneau, and T. J. Gmitter, *Appl. Phys. Lett.* **62**, 131 (1993).
- [11] L. Huld, *Phys. Stat. Sol. (a)* **8**, 173 (1971).
- [12] M. A. Green, *IEEE Trans. Electron Devices* **ED-31**, 671 (1984).
- [13] The defect-assisted Shockley-Read-Hall recombination “W. Shockley and J. W. T. Read, *Phys. Rev.* **87**, 835 (1952)” is not considered
- [14] O. D. Miller, E. Yablonovitch, and S. R. Kurtz(2011), <http://arxiv.org/abs/1106.1603>.
- [15] T. Tiedje, E. Yablonovitch, G. Cody, and B. Brooks, *IEEE Transactions on Electron Devices* **ED-31**, 711 (1984).
- [16] “Reference solar spectral irradiance: Air mass 1.5,” <http://rredc.nrel.gov/solar/spectra/am1.5/>.
- [17] See Supplemental Materials for additional data and details of the calculations.
- [18] L. Hedin, *Phys. Rev.* **139**, A796A823 (1965).
- [19] M. S. Hybertsen and S. G. Louie, *Phys. Rev. Lett.* **55**, 1418 (1985).
- [20] W. G. Aulbur, L. Jansson, and J. W. Wilkins, *Solid State Physics* **54**, 1 (1999).
- [21] G. Onida, L. Reining, and A. Rubio, *Rev. Mod. Phys.* **74**, 601 (2002).
- [22] J. Heyd, G. E. Scuseria, and M. Ernzerhof, *J. Chem. Phys.* **124**, 219906 (2006).
- [23] F. Fuchs, J. Furthmüller, F. Bechstedt, M. Shishkin, and G. Kresse, *Phys. Rev. B* **76**, 115109 (2007).
- [24] C. Rödl, F. Fuchs, J. Furthmüller, and F. Bechstedt, *Phys. Rev. B* **79**, 235114 (2009).
- [25] J. L. Shay and J. H. Wernick, *Ternary Chalcopyrite Semiconductors: Growth, Electronic Properties, and Applications* (Elsevier, 1975).
- [26] “Springer materials: The landolt-börnstein database,” <http://www.springermaterials.com/navigation>.
- [27] The remaining 42 are either metallic or with a band gap type that can not specified due to the change of orbital occupation numbers in GW calculation and are not shown.
- [28] G. A. van Vechten, “Handbook of semiconductors,” (North Holland, Amsterdam, 1980) p. 1.
- [29] S. B. Zhang, S.-H. Wei, and A. Zunger, *J. Appl. Phys.* **83**, 3192 (1998).
- [30] H. Kawazoe, M. Yasukawa, H. Hyodo, M. Kurita, H. Yanagi, and H. Hosono, *Nature* **389**, 939 (1997).
- [31] X. Nie, S.-H. Wei, , and S. B. Zhang, *Phys. Rev. Lett.* **88**, 066405 (2002).
- [32] As pointed out in J. Vidal, S. Botti, P. Olsson, J.-F. Guillemoles, and L. Reining, *Phys. Rev. Lett.* **104**, 056401 (2010) the band gaps of CuInSe<sub>2</sub> and CuInS<sub>2</sub> are very sensitive to anion displacement  $u$ . The gap calculated here corresponds to  $u = 0.239$  for CuInSe<sub>2</sub> and 0.245 for CuInS<sub>2</sub>
- [33] M. A. Green, K. Emery, Y. Hishikawa, W. Warta, and E. D. Dunlop, *Prog. Photovolt: Res. Appl.* **19**, 565 (2011).
- [34] C. Champness, “Proceedings of the 29th iee conference,” (Piscataway, 2002) p. 732.

- [35] J. A. M. AbuShama, S. Johnston, T. Moriarty, G. Teeter, K. Ramanathan, and R. Noufi, *Prog. Photovolt: Res. Appl.* **12**, 39 (2004).
- [36] A. M. Abo El Soud, T. A. Hendia, L. I. Soliman, H. A. Zayed, and M. A. Kenawy, *J. Mater. Sci.* **28**, 1182 (1993).
- [37] M. S. Reddy, K. R. Reddy, O. M. Hussaina, and P. Reddy, *Thin Solid Films* **292**, 14 (1997).
- [38] *J. Phys. Chem. Solids* **64**, 1839 (2003).
- [39] P. P. Ramesh, O. Hussain, S. Uthanna, and B. S. Naidu, *Materials Letters* **34**, 217 (1998).
- [40] A. Jagomägi, J. Krustok, J. Raudoja, M. Grossberg, I. Oja, M. Krunks, and M. Danilson, *Thin Solid Films* **480-481**, 246 (2005).
- [41] M. R. A. Bhuiyan and S. M. F. Hasan **39**, 4935 (2006).
- [42] J. Krustok, A. Jagomägi, M. Grossberg, J. Raudoja, and M. Danilson, *Solar Energy Materials & Solar Cells* **90**, 1973 (2006).
- [43] The Cu-Tl<sup>3+</sup>-VI compounds (e.g., CuTlSe<sub>2</sub>,  $E_g = 0.14$  and  $\eta \sim 0\%$ , not shown in Fig.4) have much lower band gap and weaker absorption near the threshold. Examination of their projected DOS reveals that the Cu 3*d* states lie around the valence band edge and Tl *p* states contribute mostly to the states near conduction band edge. Hence the larger proportion of the Cu<sup>1+</sup> in Cu<sub>*p*</sub>Tl<sub>*q*</sub><sup>1+</sup>VI<sub>*r*</sub> compounds (e.g,  $p = 7$  and  $p/r = 1.75$  in Cu<sub>7</sub>TlS<sub>4</sub>, relative to  $p = 1$  and  $p/r = 0.5$  in CuTlSe<sub>2</sub>) due to the lower oxidation state of Tl leads to higher joint DOS and hence higher onset absorption and higher SLME.
- [44] It should be understood that the efficiency of a solar cell may be affected by other extrinsic conditions such as defects, dopability, mobility, manufacturability and cost, and that these factors will have to be examined on a case by case basis once the broad range of candidate inorganic absorbers has been narrowed down by methodologies such as that described here.